www.elsevier.nl/locate/jorganchem

Journal of Organometallic Chemistry 604 (2000) 267–272

# Structures and spectroelectrochemistry (UV–vis, IR, EPR) of complexes $[(OC)_3ClRe]_n(abpy)$, $n = 1, 2$; abpy = 2,2′-azobispyridine

Heiko Hartmann [a], Thomas Scheiring [a], Jan Fiedler [b], Wolfgang Kaim [a],*

[a] *Institut für Anorganische Chemie, Universität Stuttgart, Pfaffenwaldring 55, D-70550 Stuttgart, Germany*
[b] *J. Heyrovsky Institute of Physical Chemistry, Academy of Sciences of the Czech Republic, Dolejškova 3, CZ-18223 Prague, Czech Republic*

Received 1 March 2000; received in revised form 25 April 2000

**Abstract**

The complexes $(OC)_3ClRe(abpy)$ (**1**) and $[(OC)_3ClRe]_2(abpy)$ (**2**) with abpy = 2,2′-azobispyridine were structurally characterized and studied by spectroelectrochemistry in the UV–vis and in the IR carbonyl stretching region. Compound **1** exhibits a *s-cis*/*E*/*s-trans* configurated abpy ligand with metal coordination to one pyridyl and one azo function and one non-bonding Re–N interaction at 3.293 Å to the second pyridyl nitrogen atom. The dinuclear complex **2** with two azoimine-coordinated metal centers is distinguished by the *trans* arrangement of the chloride ligands with respect to the $Re_2$(μ-abpy) plane, the Re–Re distance is 5.033(7) Å. The azo bond lengths at 1.272(9) (**1**) and 1.304(10) Å (**2**) indicate substantial π back donation from the rhenium(I) centers into the π*(abpy) orbital. Spectroelectrochemistry reveals the successive occupation of the π*(abpy) orbital by electrons; metal-to-ligand charge transfer features are shifted to higher energies and carbonyl stretching bands to lower wavenumbers. The EPR spectra of both radical anion intermediates $\mathbf{1}^{\bullet -}$ and $\mathbf{2}^{\bullet -}$ are dominated by very similar $^{185,187}$Re hyperfine splitting, ruling out a mixed-valent formulation. The second electron uptake is followed by the rapid loss of one chloride, leading to an unsymmetrical species in the dinuclear system. © 2000 Elsevier Science S.A. All rights reserved.

*Keywords:* Azo ligands; Crystal structure; Dinuclear complex; Rhenium compounds; Spectroelectrochemistry

## 1. Introduction

Occupation of low-lying π*(N^N) orbitals during the reduction (1) or metal-to-ligand charge transfer excitation (2) of complexes $(OC)_3XRe(N^\wedge N)$ (N^N = α-diimine or related chelate ligand, X = halogen) has been much studied [1–14] in the context of photo- or electrocatalyzed $CO_2$ reduction which involves labilization of the halide ligand as a crucial step [2,3,8,12,14].

$$(OC)_3ClRe^{I}(N^\wedge N) + e^- \rightarrow [(OC)_3ClRe^{I}(N^\wedge N^{-I})]^{\bullet -} \quad (1)$$

$$(OC)_3ClRe(N^\wedge N) \xrightarrow[\text{MLCT}]{h\nu} [(OC)_3ClRe^{II}(N^\wedge N^{-I})]^* \quad (2)$$

Ligands N^N with especially low lying π*(N^N) orbitals are those containing the azoimino function N=N–C=N, such as 2-phenylazopyridine (pap) [15,16], 3,6-bis(2-pyridyl)-1,2,4,5-tetrazine (bptz) [17–19] or 2,2′-azobispyridine (abpy) [18–23]. The latter can form dinuclear complexes with $(OC)_3ClRe$ complex fragments as previously shown [4,6]; in this work we report the isolation and structural characterization of the mononuclear $(OC)_3ClRe(abpy)$ (**1**) and of the dinuclear $[(OC)_3ClRe]_2$(μ-abpy) (**2**) with *trans* configuration of the chloride ligands.

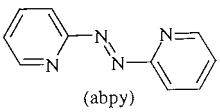
(abpy)

Both **1** and **2** were also studied by spectroelectrochemistry in the UV–vis and in the middle IR region. The complex $(OC)_3BrRe(abpy)$ related to **1** has been studied before [11] by UV–vis/IR spectroelectrochemistry. We also compare the EPR results for $\mathbf{1}^{\bullet -}$ with those of previously reported $\mathbf{2}^{\bullet -}$ [4,6].

---

* Corresponding author. Tel.: +49-711-6854170/71; fax: +49-711-6854165.
*E-mail address:* kaim@iac.uni-stuttgart.de (W. Kaim).

0022-328X/00/$ - see front matter © 2000 Elsevier Science S.A. All rights reserved.
PII: S0022-328X(00)00282-5

## 2. Results and discussion

### 2.1. Structures

The mononuclear **1** was obtained by briefly reacting $(OC)_5ClRe$ with abpy. Both **1** and **2** are air-stable compounds which could by crystallized for structure determination; the results are summarized in Tables 1–3 and illustrated in Figs. 1 and 2.

Compound **1** exhibits a bonding pattern and abpy conformation familiar from previously characterized $(OC)_4Mo(abpy)$ [21]. The versatile [18] abpy ligand adopts a *s-cis/E/s-trans* conformation with metal coordination to one pyridyl and one azo function. The bonds to the better σ-donating pyridyl and better π-accepting azo nitrogen atoms are of equal length. As in $(OC)_4Mo(abpy)$ [21] there is one non-bonding interaction at 3.293 Å from the metal to the second pyridyl nitrogen atom which suggests that the twist of the uncoordinated pyridyl ring py′ is mainly caused to minimize repulsion (which would be larger with the CH group pointing towards the metal); at the same time,

Table 1
Crystallographic data and refinement parameters for compounds **1** and **2** [a]

| | $(OC)_3ClRe(abpy)$ (**1**) | $[(OC)_3ClRe]_2(abpy)$ (**2**) |
|---|---|---|
| Empirical formula | $C_{13}H_8ClN_4O_3Re$ | $C_{16}H_8Cl_2N_4O_6Re_2$ |
| Formula weight | 489.88 | 795.56 |
| Crystal size (mm) | 0.4 × 0.3 × 0.3 | 0.3 × 0.2 × 0.2 |
| Temperature (K) | 173(2) | 173(2) |
| Space group | *C*2/*c* | $P2_1/c$ |
| Unit cell dimensions | | |
| *a* (Å) | 13.315(3) | 6.3904(13) |
| *b* (Å) | 9.0032(18) | 11.908(2) |
| *c* (Å) | 12.197(2) | 13.654(3) |
| α (°) | 90.00 | 90.00 |
| β (°) | 98.21(3) | 97.01(3) |
| γ (°) | 90.00 | 90.00 |
| *V* (Å$^3$) | 1447.2(5) | 1031.3(4) |
| *Z* | 4 | 2 |
| $D_{calc}$ (g cm$^{-3}$) | 2.248 | 2.562 |
| Absorption coefficient (cm$^{-1}$) | 0.8598 | 0.1203 |
| 2θ Range (°) | 5.48–60.02 | 4.56–60.00 |
| Index ranges | $-18 \leq h \leq 11$, $-11 \leq k \leq 12$, $-17 \leq l \leq 17$ | $-1 \leq h \leq 8$, $-1 \leq k \leq 16$, $-19 \leq l \leq 19$ |
| Reflections collected | 4849 | 4058 |
| No. unique reflections | 3294 | 2999 |
| *R* (merge) | 0.0351 | 0.0436 |
| GOF ($F^2$) [b] | 1.068 | 1.132 |
| Data/restraints/parameters | 3294/2/200 | 2999/0/112 |
| *R* indices (all data) [c,d] | $R_1 = 0.0364$, $wR_2 = 0.0945$ | $R_1 = 0.0492$, $wR_2 = 0.1144$ |
| Largest residual density (e/Å$^3$) | 0.2473 | 0.4226 |

[a] All structures were obtained on a Siemens four-circle diffractometer P4, graphite monochromated Mo–$K_\alpha$ radiation ($\lambda = 0.71073$ Å).

[b] $GOF = \{\Sigma w(|F_o|^2 - |F_c|^2)^2/(n-m)\}^{1/2}$ where $n$ = number of data and $m$ = number of variables.

[c] $R = (\Sigma||F_o| - |F_c||)/\Sigma|F_o|$.

[d] $R_w = \{\Sigma[w(|F_o|^2 - |F_c|^2)^2]/\Sigma[w(F_o^4)]\}^{1/2}$.

Table 2
Selected bond lengths (Å) and angles (°) of $(OC)_3ClRe(abpy)$ (**1**)

| | | | |
|---|---|---|---|
| *Bond lengths* | | | |
| Re–C(11) | 1.916(14) | N(1)–C(1) | 1.337(11) |
| Re–C(13) | 1.918(8) | N(2)–N(3) | 1.272(9) |
| Re–C(12) | 1.941(8) | N(2)–C(1) | 1.444(13) |
| Re–N(3) | 2.143(5) | N(3)–C(6) | 1.441(13) |
| Re–N(1) | 2.145(6) | C(11)–O(11) | 1.156(16) |
| Re–Cl | 2.475(4) | C(12)–O(12) | 1.133(10) |
| | | C(13)–O(13) | 1.152(12) |
| *Bond angles* | | | |
| C(11)–Re–N(3) | 93.5(3) | N(3)–Re–Cl | 85.3(2) |
| C(12)–Re–N(3) | 101.4(3) | C(11)–Re–C(12) | 86.5(4) |
| C(13)–Re–N(3) | 169.8(4) | C(13)–Re–C(12) | 88.4(4) |
| C(11)–Re–N(1) | 97.3(3) | C(11)–Re–C(13) | 90.0(4) |
| C(12)–Re–N(1) | 173.1(3) | O(11)–C(11)–Re | 177.9(9) |
| C(13)–Re–N(1) | 97.4(3) | O(12)–C(12)–Re | 178.4(8) |
| N(1)–Re–Cl | 84.9(2) | O(13)–C(13)–Re | 176.4(9) |
| N(3)–Re–N(1) | 72.7(3) | N(1)–C(1)–N(2) | 117.4(9) |
| C(11)–Re–Cl | 177.0(3) | C(1)–N(2)–N(3) | 112.3(7) |
| C(13)–Re–Cl | 91.7(3) | C(1)–N(1)–Re | 115.8(6) |
| C(12)–Re–Cl | 91.1(3) | N(2)–N(3)–Re | 121.5(6) |

Table 3
Selected bond lengths (Å) and angles (°) of $[(OC)_3ClRe]_2(abpy)$ (**2**)

| | | | |
|---|---|---|---|
| *Bond lengths* | | | |
| Re(1)–C(2) | 1.928(7) | C(1)–O(1) | 1.139(8) |
| Re(1)–C(3) | 1.930(7) | C(2)–O(2) | 1.160(9) |
| Re(1)–C(1) | 1.937(6) | C(3)–O(3) | 1.129(9) |
| Re(1)–N(2) | 2.135(5) | N(2)–C(01) | 1.361(7) |
| Re(1)–N(1) | 2.134(6) | C(01)–N(1A) | 1.409(7) |
| Re(1)–Cl(1) | 2.4587(18) | N(1)–N(1A) | 1.304(10) |
| *Bond angles* | | | |
| C(2)–Re(1)–C(3) | 90.5(3) | N(2)–Re(1)–Cl(1) | 82.35(14) |
| C(2)–Re(1)–C(1) | 86.5(3) | N(1)–Re(1)–Cl(1) | 86.00(14) |
| C(3)–Re(1)–C(1) | 92.3(3) | C(2)–Re(1)–Cl(1) | 91.1(2) |
| C(2)–Re(1)–N(2) | 98.2(2) | C(3)–Re(1)–Cl(1) | 178.2(2) |
| C(3)–Re(1)–N(2) | 98.3(2) | O(1)–C(1)–Re(1) | 176.7(6) |
| C(1)–Re(1)–N(2) | 168.4(2) | O(2)–C(2)–Re(1) | 178.4(7) |
| C(2)–Re(1)–N(1) | 170.7(2) | O(3)–C(3)–Re(1) | 176.8(7) |
| C(3)–Re(1)–N(1) | 92.6(2) | N(1A)–N(1)–C(01A) | 114.0(6) |
| C(1)–Re(1)–N(1) | 102.2(2) | N(1A)–N(1)–Re(1) | 118.9(5) |
| N(2)–Re(1)–N(1) | 72.63(18) | C(01A)–N(1)–Re(1) | 126.6(4) |
| C(1)–Re(1)–Cl(1) | 86.96(19) | N(2)–C(01)–N(1A) | 115.3(5) |

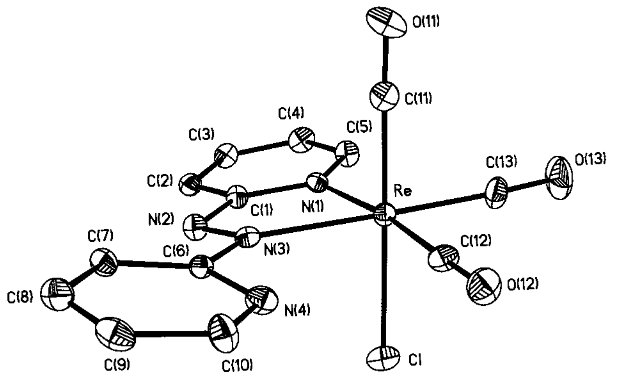

Fig. 1. Molecular structure of compound **1** in the crystal.

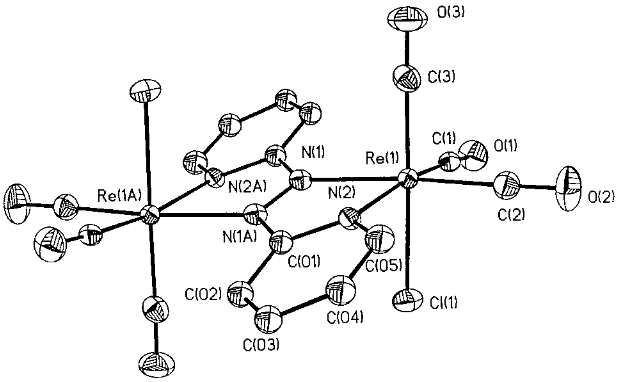

Fig. 2. Molecular structure of compound **2** in the crystal.

Table 4
Spectroelectrochemical data for the reduction of **1** and **2** [a]

| | $\mathbf{1}^n$ | $\mathbf{2}^n$ |
|---|---|---|
| $E$ (red 1) [b] | $-0.78$ ($E_{1/2}$) | 0.00 ($E_{1/2}$), 0.34 ($E_{1/2}$) [d] |
| $E$ (red 2) [b] | $-1.54$ ($E_{pc}$) | $-0.80$ ($E_{1/2}$), $-0.56$ ($E_{1/2}$) [d] |
| $\nu_{CO}$ [c] ($n=0$) | 2030vs, 1943s, 1917s | 2044w, 2010vs, 1960sh, 1938m |
| $\nu_{CO}$ ($n=-1$) | 2004vs, 1898s, 1866s | 2017w, 2005s, 1909s, 1885sh |
| $\nu_{CO}$ ($n=-2$) [d] | n.a. | 1999m, 1989s, 1877s, 1858sh [f] |
| $\lambda_{max}/\varepsilon$ [e] ($n=0$) | 565/2.68, 360/6.72 (MLCT) | 788/10.99, 710sh, 404/11.10 (MLCT), 332/12.80 (IL) |
| $\lambda_{max}/\varepsilon$ ($n=-1$) | 502/2.20 (MLCT), 392/10.08 (IL) | 631/3.40, 532sh, 497/7.20 (MLCT), 382/13.70 (IL) |
| $\lambda_{max}/\varepsilon$ ($n=-2$) [d] | 440/2.20, 320/6.30 (IL) | 546sh, 507/8.00, 483/8.10, 392sh (IL) |

[a] Measurements in $CH_2Cl_2$/0.1 M. $Bu_4NPF_6$ ($\mathbf{1}^n$) or 1,2-dichloroethane /0.1 M $Bu_4NPF_6$ ($\mathbf{2}^n$).

[b] Potentials in V vs. $(C_5H_5)_2Fe^{+/0}$, half-wave ($E_{1/2}$) or cathodic peak potentials ($E_{pc}$) for irreversible processes.

[c] Carbonyl stretching bands in $cm^{-1}$.

[d] Chloride-free species, see text.

[e] Absorption maxima ($\lambda_{max}$) in nm; molar extinction coefficients ($\varepsilon$) in $10^3$ $M^{-1}$ $cm^{-1}$.

[f] Pyridyl ring vibrations at 1610 and 1482 $cm^{-1}$, see text.

this arrangement ensures π conjugation through approximate planarity of coordinated abpy, the dihedral angle beetwen the planes of py′ and the rest of coordinated abpy is 16.1°.

The dinuclear complex **2** with two azoimine-coordinated metal centers at virtually identical Re–N bond lengths is distinguished by the *trans* arrangement of the chloride ligands with respect to the approximately planar $Re_2$(μ-abpy) moiety. The Re–Re distance is 5.033(7) Å and there is a slight twisting of the abpy ligand as illustrated by the torsional angle of 17.7° for Re(1)–C(1)–N(1)–C(1A).

It is the first time that such a positional isomer could be structurally identified. The preference for this isomer (there is only one detectable by NMR) is not immediately obvious, apart from the higher symmetry and resulting absence of a dipole moment; a *cis* isomer should not be disfavored on steric reasons. In any case there has to be conformational reorganization of the abpy ligand on the way from the free ligand (*s-trans*/*E*/*s-trans* [22,24]) via the mononuclear **1** (*s-cis*/*E*/*s-trans*) to the dinuclear **2** (*s-cis*/*E*/*s-cis*).

The azo bond lengths at 1.272(9) Å (**1**) and 1.304(10) Å (**2**) indicate substantial π back donation from the rhenium(I) centers into the π*(abpy) orbital. Such effects have been noted previously for a dicopper(I) compound of abpy [21] and for various complexes of pap [15,16]; however, the value for **2** with its large deviation from that of free abpy at 1.246(2) Å [24] and its closeness to the 1.345(7) Å of one-electron reduced 2,2′-azobispyrimidine in a dicopper(I) complex [25] illustrate the large amount of metal-to-ligand π electron shift in the ground state. It is interesting to note that non-organometallic rhenium(III) fragments such as $Cl_3(Ph_3PO)Re$ induce similar lengthening of N–N bonds in complexes of 2-phenylazopyridine ligands [16].

### 2.2. Reduction of **1** and **2**

Compound **1** shows the conventional [7,9–13] electrochemical behavior for complexes $(N{^\wedge}N)Re(CO)_3Cl$, i.e. a reversible one-electron uptake followed by a completely irreversible step (loss of chloride; Table 4). Complex **2** was reinvestigated [20] by cyclic voltammetry at varying scan rates to reveal a similar pattern, however, the loss of chloride after the second reduction was found to be slower than for system $\mathbf{1}^{n-}$. Accordingly, half-wave potentials could be determined both for the systems $\mathbf{2}^{0/-/2-}$ and for $[\mathbf{2}\text{-}Cl^-]^{+/0/-}$, $[\mathbf{2}\text{-}Cl^-]$ = $\{[(OC)_3Re](abpy)[ReCl(CO)_3]\}$ (Table 4). The case for dissociation of only one chloride ligand in $\mathbf{2}^{2-}$ is made by IR spectroelectrochemistry (cf. below). The EPR experiments in dichloromethane or 1,2-dichloroethane/0.1 M $Bu_4NPF_6$ gave spectra with partially resolved metal hyperfine splitting [4,6], ligand HFS was not resolved due to the large line widths of

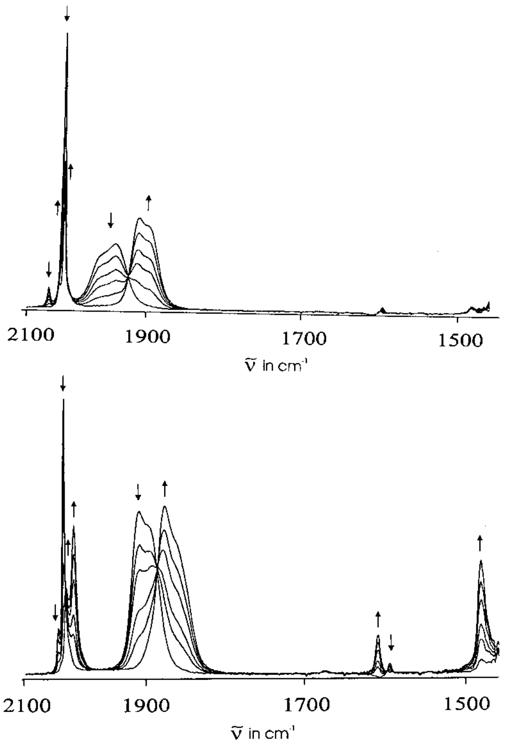

Fig. 3. IR spectroelectrochemistry of $\mathbf{2}^{0/-}$ (top) and $\mathbf{2}^{-}$/[$\mathbf{2}$-Cl$^{-}$]$^{-}$ (bottom) in 1,2-dichloroethane/0.1 M $Bu_4NPF_6$.

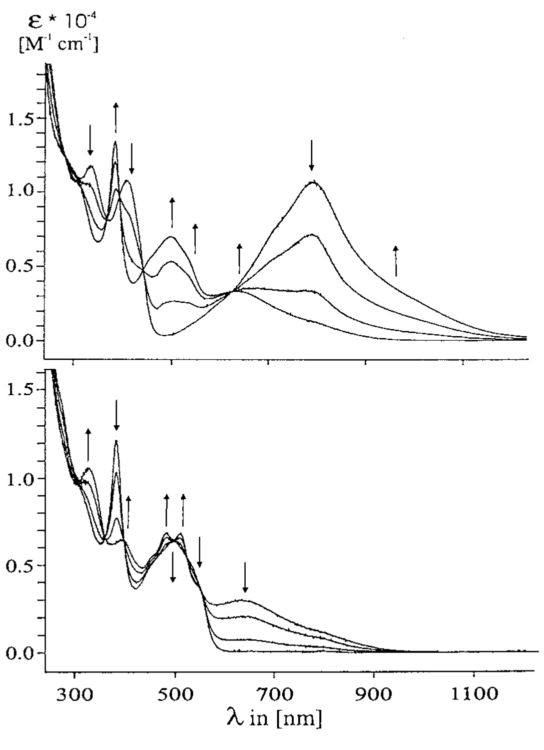

Fig. 4. UV–vis spectroelectrochemistry of $\mathbf{2}^{0/-}$ (top) and $\mathbf{2}^{-}$/[$\mathbf{2}$-Cl$^{-}$]$^{-}$ (bottom) in 1,2-dichloroethane/0.1 M $Bu_4NPF_6$.

about 0.2 mT. The EPR studies reveal that both radical anions $\mathbf{1}^{\bullet-}$ ($g = 2.0041$) and $\mathbf{2}^{\bullet-}$ ($g = 2.0039$) have the spin predominantly in the π*(abpy) MO, the large $^{185,187}$Re ($I = 5/2$) coupling constants of 2.38 mT ($\mathbf{1}^{\bullet-}$, six lines, 1 Re) and 2.54 mT ($\mathbf{2}^{\bullet-}$, 11 lines, 2 Re) [4,6] notwithstanding (complex $[(bpy)ReCl(CO)_3]^{\bullet-}$ has a (Re) = 1.2 mT [4]). The close similarity of the metal coupling constants of $\mathbf{1}^{\bullet-}$ and $\mathbf{2}^{\bullet-}$ is in agreement with the radical ligand [26] formulation; a delocalized mixed-valent situation would produce only half the coupling constant in the dinuclear system [27,28].

Spectroelectrochemistry in the UV–vis and IR regions using an OTTLE cell [29] was further employed to elucidate the response of the two compounds towards electron uptake. The results are summarized in Table 4; Figs. 3 and 4 show the response of **2**.

Complex **1** shows essentially the same behavior as $(OC)_3BrRe(abpy)$ [11] (Table 4). The dinuclear **2** exhibits a weak carbonyl stretching band at high energies in the IR spectrum, in addition to the three more intense features typical [11] for a *fac*-$(OC)_3Re$ moiety.

The uniform low-energy shifts of $\nu_{CO}$ are as expected [7,11], reflecting the charge effect [30] rather than ligand-to-metal electron transfer. It is remarkable, however, that only after the chemically irreversible second reduction the typical bands for pyridyl vibrations emerge at 1610 and 1482 cm$^{-1}$ (Fig. 3). This observation strongly suggests the loss of inversion symmetry through dissociation of only one chloride from $\mathbf{2}^{2-}$ to produce the species [$\mathbf{2}$-Cl$^{-}$]$^{-}$ = $\{[(OC)_3Re^{I}](abpy^{-II})[Re^{I}Cl(CO)_3]\}^{-}$; according to the selection rules for IR spectroscopy, the vibrations must be accompanied by a change in the dipole moment to exhibit well observable bands. The centrosymmetric **2** and $\mathbf{2}^{\bullet-}$, on the other hand, exhibit only very small pyridyl ring vibration bands at 1598 and 1482 cm$^{-1}$. The small shift of the high-energy ring vibration to higher energies on reduction (Fig. 3) is compatible with the notion of an azo-centered orbital π*(abpy) [31]. Apparently, the loss of chloride does not produce essentially different CO stretching vibrations, a splitting of the corresponding bands could not be detected. The stability of pentacoordinate tricarbonylrhenium(I) centers is not unexpected [7,11] and has precedents in tricarbonylmanganese chemistry [32]; hydrazido ligands as in abpy$^{2-}$ are very electron rich ($\sigma + \pi$) [33] and can thus well stabilize a 16 valence electron situation. Obviously, the dissociation of only one chloride ion in system **2** is sufficient to stabilize the doubly reduced state.

UV–vis spectroelectrochemistry as shown in Fig. 4 for dinuclear **2** exhibits the expected intensity decrease and high-energy shift of the long-wavelength metal-to-ligand charge transfer (MLCT) band (Table 4). In addition, the one-electron reduced species $\mathbf{1}^{\bullet-}$ and $\mathbf{2}^{\bullet-}$

exhibit the typical narrow intra-ligand (IL) bands of azoaromatic radical anions at about 390 nm; for instance, the *E*-azobenzene anion has $\lambda_{max}$ at 430 nm [34]. After dissociation of one chloride ion, the resulting species still show intense absorption in the visible which may be tentatively assigned to IL transitions: Loss of chloride causes a destabilization of π*(abpy) as evident from anodically shifted potentials (Table 4); this destabilization would lower the energy of IL transitions.

## 3. Experimental

### 3.1. Syntheses

#### 3.1.1. 2,2′-(Azobispyridine)(tricarbonyl)chlororhenium (1)

An amount of 240 mg (0.66 mmol) $Re(CO)_5Cl$ and 120 mg (0.66 mmol) abpy [19] was heated to reflux for 20 min in 40 ml of a 3:1 toluene–dichloromethane mixture. The deep blue solution was concentrated to 20 ml, treated with 5 ml pentane and cooled to 4°C. After 24 h a deep blue precipitate was collected, washed with diethyl ether and dried to yield 249 mg (78%). Anal. Calc. for $C_{13}H_8ClN_4O_3Re$: C, 31.87; H, 1.65; N, 11.44. Found C, 31.85; H, 1.50; N, 11.45%. $^1$H-NMR ($CD_2Cl_2$): $\delta = 7.66$ (ddd, 1H, $H^{5'}$), 7.72 (ddd, 1H, $H^5$), 8.05 (ddd, 1H, $H^{4'}$), 8.15 (dt, 1H, $H^{3'}$), 8.29 (td, 1H, $H^4$), 8.71 (ddd, 1H, $H^3$), 8.83 (ddd, 1H, $H^{6'}$), 9, 12 (ddd, 1H, $H^6$), ppm. $^3J(H^3H^4) = 8.0$ Hz, $^4J(H^3H^5) = 1.3$ Hz, $^5J(H^3H^6) = 0.7$ Hz, $^3J(H^4H^5) = 7.8$ Hz, $^4J(H^4H^6) = 1.6$ Hz, $^3J(H^5H^6) = 5.3$ Hz, $^3J(H^{3'}H^{4'}) = 8.2$ Hz, $^4J(H^{3'}H^{5'}) = 1.0$ Hz, $^5J(H^{3'}H^{6'}) = 1.0$ Hz, $J(H^{4'}H^{5'}) = 7.8$ Hz, $^4J(H^{4'}H^{6'}) = 1.6$ Hz, $^3J(H^{5'}H^{6'}) = 4.8$ Hz.

Deep blue crystals for X-ray diffraction were obtained through slow evaporation of a $CH_2Cl_2$ solution.

Complex **2** was obtained as previously described [20]. Deep green single crystals suitable for X-ray diffraction were obtained from a saturated solution in acetone through layering with *n*-pentane.

### 3.2. Instrumentation

EPR spectra were recorded in the X band on a Bruker System ESP 300 equipped with a Bruker ER035M gaussmeter and a HP 5350B microwave counter. $^1$H-NMR spectra were taken on a Bruker AC 250 spectrometer; IR spectra were obtained using Perkin–Elmer 684 and 283 instruments. UV–vis/NIR absorption spectra were recorded on a Bruins Instruments Omega 10 spectrophotometer. Cyclic voltammetry was carried out in 0.1 M $Bu_4NPF_6$ solutions using a three-electrode configuration (glassy carbon electrode, Pt counter electrode, Ag/AgCl reference) and a PAR 273 potentiostat and function generator. The ferrocene/ferrocenium couple served as internal reference. Spectroelectrochemical measurements were performed using an optically transparent thin-layer electrode (OTTLE) cell [29] for UV–vis spectra and a two-electrode capillary for EPR studies [35].

### 3.3. Crystallography

The structures of **1** and **2** were solved by the Patterson method. The refinement was carried out employing full matrix least-squares method [36]. Absorption correction ($\psi$-scan) did not improve *R* values or standard deviations. All non-hydrogen atoms were refined anisotropically. The hydrogen atoms were introduced at proper geometric positions and treated according to the riding model with isotropic thermal parameters fixed at 20% greater than that of the bonded atom. Anisotropic thermal parameters were refined for all non-hydrogen atoms.

## 4. Supplementary material

Crystallographic data for the structural analysis have been deposited with the Cambridge Crystallographic Data Centre, CCDC-140132 and -140133 for compounds **1** and **2**, respectively. Copies of the information may be obtained free of charge from: The Director, CCDC, 12 Union Road, Cambridge, CB2 1EZ, UK (fax: +44-1223-336033; e-mail: deposit@ccdc.cam.ac.uk; www: http://www.ccdc.cam.ac.uk).

## References

[1] P.J. Giordano, M.S. Wrighton, J. Am. Chem. Soc. 101 (1979) 2888.
[2] B.P. Sullivan, T.J. Meyer, J. Chem. Soc. Chem. Commun. (1984) 1244.
[3] J. Hawecker, J.M. Lehn, R. Ziessel, Helv. Chim. Acta 69 (1986) 1900.
[4] W. Kaim, S. Kohlmann, Chem. Phys. Lett. 3 (1987) 365.
[5] W. Kaim, H.E.A. Kramer, C. Vogler, J. Rieker, J. Organomet. Chem. 367 (1989) 107.
[6] W. Kaim, S. Kohlmann, Inorg. Chem. 29 (1990) 2909.
[7] A. Klein, C. Vogler, W. Kaim, Organometallics 15 (1996) 236.
[8] T. Scheiring, A. Klein, W. Kaim, J. Chem. Soc. Perkin Trans. 2 (1997) 2569.
[9] G.J. Stor, F. Hartl, J.W.M. van Outersterp, D.J. Stufkens, Organometallics 14 (1995) 1115.
[10] R.R. Andrea, W.G.J. de Lange, T. van der Graf, M. Rijkhoff, D.J. Stufkens, A. Oskam, Organometallics 7 (1988) 1100.
[11] G.J. Stor, F. Hartl, J.W.M. van Outersterp, D.J. Stufkens, Organometallics 14 (1985) 1115.
[12] F.P.A. Johnson, M.W. George, F. Hartl, J.J. Turner, Organometallics 15 (1996) 3374.
[13] B.D. Rossenaar, F. Hartl, D.J. Stufkens, Inorg. Chem. 35 (1996) 6194.

[14] R. Ziessel, in: K. Kalyanasundaram, M. Grätzel (Eds.), Photosensitization and Photocatalysis Using Inorganic and Organometallic Compounds, Kluwer, Dordrecht, 1993, p. 217.
[15] (a) R.A. Krause, K. Krause, Inorg. Chem. 21 (1987) 1. (b) T. Bao, K. Krause, R.A. Krause, Inorg. Chem. 27 (1988) 759.
[16] S. Banerjee, S. Bhattacharyya, B.K. Dirghangi, M. Menon, A. Chakravorty, Inorg. Chem. 39 (2000) 6.
[17] M. Schwach, H.-D. Hausen, W. Kaim, Inorg. Chem. 38 (1999) 2242.
[18] D.A. Baldwin, A.B.P. Lever, R.V. Parish, Inorg. Chem. 8 (1969) 107.
[19] S. Kohlmann, S. Ernst, W. Kaim, Angew. Chem. 97 (1985) 698; Angew. Chem. Int. Ed. Engl. 24 (1985) 684.
[20] W. Kaim, S. Kohlmann, Inorg. Chem. 26 (1987) 68.
[21] W. Kaim, S. Kohlmann, J. Jordanov, D. Fenske, Z. Anorg. Allg. Chem. 598–599 (1991) 217.
[22] M. Krejcik, S. Zalis, J. Klima, D. Sykora, W. Matheis, A. Klein, W. Kaim, Inorg. Chem. 32 (1993) 3362.
[23] J. Fees, H.-D. Hausen, W. Kaim, Z. Naturforsch. Teil. b 50 (1995) 15.
[24] (a) R. Schäfer, W. Kaim, J. Fiedler, Inorg. Chem. 32 (1993) 3199. (b) H. Bock, R. Dienelt, H. Schödel, T.T.H. Van, Struct. Chem. 9 (1998) 279.
[25] N. Doslik, T. Sixt, W. Kaim, Angew. Chem. 110 (1998) 2125; Angew. Chem. Int. Ed. Engl. 37 (1998) 2403.
[26] W. Kaim, Coord. Chem. Rev. 76 (1987) 187.
[27] R. Gross, W. Kaim, Inorg. Chem. 25 (1986) 4865.
[28] W. Kaim, W. Bruns, J. Poppe, V. Kasack, J. Molec. Struct. 292 (1993) 221.
[29] (a) M. Krejcik, A.A. Vlcek, J. Electroanal. Chem. Interfacial Electrochem. 313 (1991) 243. (b) M. Krejcik, M. Danek, F. Hartl, J. Electroanal. Chem. Interfacial Electrochem. 317 (1991) 179.
[30] W. Kaim, W. Bruns, S. Kohlmann, M. Krejcik, Inorg. Chim. Acta 229 (1995) 143.
[31] W. Kaim, S. Kohlmann, Inorg. Chem. 25 (1986) 3442.
[32] F. Hartl, A. Vlcek Jr., L.A. deLearie, C.G. Pierpont, Inorg. Chem. 29 (1990) 1073.
[33] R. Gross, W. Kaim, J. Chem. Soc. Faraday Trans. 1 83 (1987) 3549.
[34] T. Shida, Electron Absorption Spectra of Radical Ions, Elsevier, Amsterdam, 1988, p. 194.
[35] W. Kaim, S. Ernst, V. Kasack, J. Am. Chem. Soc. 112 (1990) 173.
[36] SHELXTLN, Version 5.1, Bruker AXS, 1998.